
Formation of Nascent Chemoautotrophic Carbon Fixation Systems under Different Redox Conditions of Fluid Degassing of the Early Earth

Sergey A. Marakushev ^{a*} and Olga V. Belonogova ^a

DOI: 10.9734/bpi/npgees/v9/7056A

ABSTRACT

In theories of the origin of life, the most reasonable is the concept of the primacy of autotrophic metabolism, in which carbon dioxide (CO₂) is considered as the only source of carbon for the functioning of nascent metabolic pathways. The aim of this paper was to demonstrate that the origin and development of primary autotrophic metabolism on early Earth were influenced by the two different regimes of degassing of the Earth – reducing (predominance CH₄) and oxidative (CO₂). It follows from this that the ancestral carbon used in metabolism may have been derived from CH₄ if the outflow of magma fluid to the surface of the Earth consisted mainly of methane. In such an environment, the primary autotrophic metabolic systems had to be methanotrophic. Due to the absence of molecular oxygen in the Archean conditions, this metabolism would have been anaerobic, i.e., oxidation of methane should have been carried out by inorganic high-potential electron acceptors. In light of the primacy and prevalence of CH₄-dependent metabolism in hydrothermal systems of the ancient Earth, we propose a model of carbon fixation where the methane is fixed/transformed in a sequence of reactions in an autocatalytic methane-fumarate cycle. Nitrogen oxides are thermodynamically most favorable among possible oxidants of methane; however, even the activity of oxygen created by mineral buffers of iron in hydrothermal conditions is sufficient for methanotrophic acetogenesis. The Hadean - Archean hydrothermal system model is considered in the form of a phase diagram, which demonstrates the area of redox and P, T conditions favorable for the formation and development of primary methanotrophic metabolism.

Keywords: Degassing of Earth; abiotic hydrocarbons; methanotrophy; acetogenesis; hydrothermal system; methane-fumarate cycle.

^a Federal Research Center for Problems of Chemical Physics and Medical Chemistry, Russian Academy of Sciences, Academician Semenov Avenue 1, Chernogolovka, Moscow Region-142432, Russian Federation.

*Corresponding author: E-mail: shukaram@yandex.ru;

1. INTRODUCTION

The fixation of inorganic carbon into organic material is the chemical basis for the functioning of the first self-reproducing C–H–O systems in submarine hydrothermal systems on ancient Earth. Favorable thermodynamic and kinetic conditions for this process were created there due to the optimal composition of minerals - catalysts and thermal and chemical gradients resulting from pulses of hydrogen degassing of the liquid earth's core and rock-water interaction. According to modern concepts, a pool of carboxylic and ketoacids - autocatalysts, was created under the hydrothermal conditions of the Archean, which self-organized into autocatalytic protometabolic networks on the surface of minerals (e.g., [1-3]). To date, the number of publications devoted to the anaerobic oxidation of hydrocarbons, found in alkanotrophic bacteria and archaea, is increasing. However, the construction of models for the origin of the primary autotrophic metabolism assimilating hydrocarbons is not given significant importance. The existing models are based mainly on the chemoautotrophic systems of carbon dioxide fixation that have been widely studied today, ignoring the high probability of its practical absence on the earth's surface during the period of the origin of life. It is erroneously believed that hydrocarbons and, in particular, methane, on Earth are of exclusively biogenic origin, neglecting their inorganic endogenous nature, which is justified in a number of our works [3-8]. The present study considers existing views on the primacy of methanotrophic metabolism and proposes a new cyclic model of it in a periodically changing Hadean-Archaean environment.

2. DEEP METHANE DEGASSING OF THE EARLY EARTH

The deep hydrocarbon generation in seismically active satellites manifested as the significant concentrations of hydrocarbons, including methane on their surface. For example, there is a prevalence of methane on Titan and Enceladus (the satellites of Saturn) [9-11] and on Europa (the satellite of Jupiter) (e.g. [12]). Additionally, high concentrations of methane are assumed to be present on early Mars [13]

On Earth, methane and other hydrocarbons are generated in magma chambers and are carried by fluids to the surface through volcanic processes, and are trapped in the gas-liquid inclusions during the minerals formation. This has been observed in the quartz–methane amygdaline inclusions that occur in the form of relics present in metamorphic-basaltic rocks of Greenland that were dated to 3.8 billion years [14]. The inclusion of hydrocarbons and reduced organic compounds in Archean quartz [14, 15] indicates a sufficiently reductive environment at this time. There is evidence that Archean atmosphere was enriched in hydrogen and methane [16,17], but the oxidation state of magma sources apparently has changed [18]. According to the trace-elements data of igneous zircons crustal origin (mainly Ce-based oxybarometer), it was shown that the Hadean continental crust was significantly more reduced than its modern counterpart and experienced progressive oxidation ~3.6 billion years ago [19, 20]. In addition, the oxygen activity (log units) in the earth's crust periodically changed with regards to

the quartz-magnetite-fayalite redox buffer from -8 to +4 in Hadean and from -7 to +7 in the early Archean. Significant fluctuations in the redox state of Archean and Hadean zircons indicate a pulsed regime of Earth degassing during this period of time, which, in our opinion, is related to impulses in the geomagnetic field [21-23]. Thus, the evolution of the Earth over a period of 4.6 billion years is determined by the impulsive degassing of its liquid core along the structures of the dislocation of its solid silicate shells (mantle and crust).

Of all the magmatic formations of the world, the alkaline magmatism is the deepest and controlled by mantle cycles [6,24] and in its magma chambers hydrocarbon substances arises. Thermodynamic calculations show the preference of deep formation and stability of hydrocarbons, which are carried in fluids to the Earth surface (temperature and pressure decreasing), are transformed to methane [25]. This is confirmed by the massive production of abiotic methane at ~40 km depth [26] and the discovered bubbles of hydrocarbons trapped in eclogite, a metamorphic rock that forms at high pressure at a depth of at least 80 km [27]. The gas-liquid inclusions of methane in diamond, geochemical analyzes and P-T experiments on the synthesis of hydrocarbons [8, 28-33] also prove its deep origin.

The global mid-ocean ridge system represents a major site for outgassing of volatiles from the earth's mantle. Methane, which was believed to have a surface origin (low-temperature serpentinization ~100° C), apparently is formed at depth, at temperatures of ca. 400° C under redox conditions characterizing intrusive rocks derived from sub-ridge melts [34]. Thus, deep, alkaline-basalt magmatism (elevated alkali content, especially K₂O), in contrast to basalt-andesitic one, is mainly responsible for methane degassing on the earth's surface. With increasing alkalinity (alkaline slope) in the fluid inclusions of igneous rocks invariably appear with different hydrocarbons [35,36]. The high content of potassium in the high-silica Hadean crust [37] indicates the depth of magmatism and its hydrocarbon specificity.

The model of two-stage development of fluids (I ↔ II) generated by the earth's core via mantle magma chambers is presented in the phase diagram of the C–H–O compositions, Fig. 1. Fluids ejected from the liquid core were initially saturated with hydrogen, with oxygenic components being of minor importance. However, during the process of the earth's silicate shells (mantle and crust) extension (associated, in our opinion, with a Hadean to Paleoproterozoic geodynamo [38], an increase of fluid permeability stimulates the selective migration of hydrogen (the most mobile component) from it. This process is responsible for hydrogen losing its leading position in ejected fluids and being fundamental to the evolution of low and normal alkalinity magmatism [5,6]. In this scenario, the fractionation of chemical components in the fluid would result in rich acidic CO₂ solutions (for example, H₂+2CO = H₂O+0.5CO₂+1.5C and H₂O+CO₂ = H₂CO₃). These solutions are widely observed in the composition of fluid inclusions in minerals of all igneous rocks of low and normal alkalinity. The water-carbonic regime of hydrogen fluid evolution is represented in the phase diagram,

Fig. 1, as an area of thermodynamic stability (facies I) limited by C–CO₂–H₂O paragenesis.

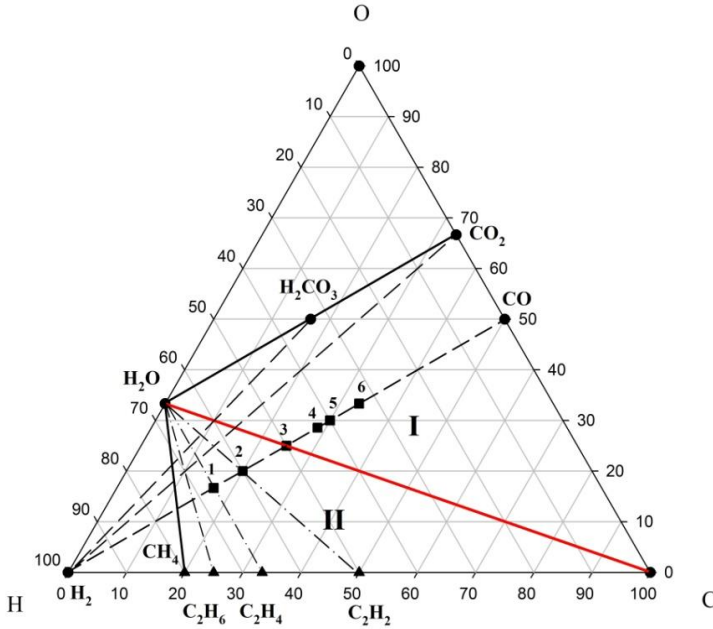


Fig. 1. Two regimes of evolution of the C–H–O system on the phase diagram of its compositions. Roman numerals denote various regimes of hydrogen fluid evolution: (I) water-carbonic and (II) water-hydrocarbon solutions, separated by H₂O–C equilibrium (red). Parageneses (assemblages) of the initial substances (H₂, CO, CO₂) are denoted by dashed sub-lines, while dash-dotted lines indicate the parageneses (C₂H₆–H₂O, C₂H₄–H₂O, etc) of hydrocarbons (black triangles) with water. Black squares denote organic substances within the two component (H₂–CO) subsystem: methanol (1), ethylene glycol (2), acetate (3), succinate (4), pyruvate (5), and fumarate (6)

The transition to compression of silicate shells prevents hydrogen migration from fluids and stimulates the production of hydrocarbons within them; for example, consider the reactions: $3\text{H}_2 + \text{CO} = \text{H}_2\text{O} + \text{CH}_4$, $5\text{H}_2 + 2\text{CO} = 2\text{H}_2\text{O} + \text{C}_2\text{H}_6$ (Fig. 1, facies II, reducing conditions). The hydrogen in the reaction like $4\text{H}_2 + \text{H}_2\text{CO}_3 = 3\text{H}_2\text{O} + \text{CH}_4$ destroys the acid components in fluids, and this determines the alkaline slope in the development of magmatism. This is a two-stage model of the development of the C–H–O system (I ↔ II), which depends on the composition of earth's core fluids, and their transformations in magma chambers.

The existing theories on the origin of autotrophic life mainly identify carbon dioxide as the unique carbon source for metabolism. This autotrophic metabolism should have originated at a high partial pressure of CO₂ in the environment (paragenesis CO₂ + H₂O, Fig. 1, facies I). We assume that in geodynamic regime II (CH₄ + H₂O paragenesis), carbon ancestral metabolism could use methane as a carbon source if the flow of free energy from the geochemical environment was coupled with biomass formation reactions. Perhaps, these different regimes of fluid degassing determined the physicochemical conditions of the ambient environment, which, in turn, provided an opportunity for the emergence and development of various systems of ancient autotrophic metabolism. In regime II (Fig. 1), methane and other hydrocarbons could be substrates of the emerging autotrophic metabolism.

The above geochemical and petrological data indicate highly heterogeneous redox conditions between the present-day Earth and conditions that periodically arose in the early Earth. We consider that the anaerobic reductive geochemical conditions of the Archean played a decisive role in the origin and development of carbon and energy metabolism, which were vastly different from those observed in the tops of the branches of the modern phylogenetic tree of prokaryotes. Most metabolically anaerobic chemoautotrophic organisms are either extinct or strongly limited to narrow anoxic ecological niches. Lateral gene transfer and subsequent phylogenetic divergence erased most evolutionary information recorded in ancestral prokaryotic genomes [39].

3. ANAEROBIC OXIDATION OF METHANE

The study of anaerobic oxidation of methane (AOM) in modern oxygen-free environments (marine sedimentary rocks, gas-hydrates, mud volcanoes, black smokers, hydrocarbon seeps) has increased in recent years [40,41]. This direction was sparked by the discovery of anaerobic methanotrophic archaea [42] and their structural consortia with sulfate-reducing bacteria [43]. A similar consortia was later discovered in archaea species that function in chemical conjunction with the bacterium *Candidatus Methyloirabilis oxyfera*, which itself can independently couple AOM to denitrification [44,45]. Furthermore, the microbiological AOM was recently shown to be directly associated with the reduction of iron and manganese compounds and minerals [46-49], as, for example, in the reaction $\text{CH}_4 + 8\text{Fe}^{3+} + 2\text{H}_2\text{O} \rightarrow \text{CO}_2 + 8\text{Fe}^{2+} + 8\text{H}^+$ ($\Delta G^0 = -454$ kJ/mol CH₄).

Recent studies have suggested that both archaea (ANME-2d) [45] and bacteria (*Methylobacter*) [50], without partners, may themselves be versatile methanotrophs capable of using different oxidants as electron acceptors under different environmental conditions. AOM occur by the reversal canonical methanogenesis pathway [51] and, perhaps, the evolution of life periodically includes forward or reverse pathways depending on the substrate (methanogen-methanotroph “switch back” [52]. For example, nickel enzyme purified from methanogenic archaea can catalyze the oxidation of methane to methyl coenzyme M ($\text{CH}_4 + \text{CoM-S-S-CoB} \rightarrow \text{CH}_3\text{-S-CoM} + \text{HS-CoB}$; $\Delta G^0 = 30 \pm 10$

kJ), that is the reverse reaction of methyl coenzyme M reductase [53]. In general, methano- and methylotrophs use different but often interrelated pathways of carbon fixation [54]. Newly described methanotrophic anaerobic prokaryotes are frequently discovered in various extreme environmental conditions [55], underscoring the functional and phylogenetic diversity of this group. The search for relict forms of anaerobic methanotrophic metabolism continues.

In 2013, Wolfgang Nitschke and Michael Russell described the possibility of methane assimilation as the sole source of carbon for primordial metabolism [56]. They suggested that methanotrophy and not methanogenesis may have been the founding metabolism in the first protocells and presented a model of methanotrophic acetogenesis in which methane, as the carbon source, is assimilated into the biomimetic analogue of the modern reverse acetyl-CoA pathway. The proposed methane oxidant in this pathway of CH₄ fixation was nitric oxide (NO), formed via nitrate/nitrite transformation ('denitrifying methanotrophic acetogenesis') [12]. The authors consider the process of low-temperature harzburgite (ophiolites) hydrothermal serpentinization in the presence of carbon oxides served as the main source of methane. Nevertheless, Wang et al. [34] argue that there is another unified deep high-temperature process of methane-making for these hydrothermal areas.

In the absence of oxygen, the methane oxidation requires electron acceptors with a high redox potential (such as nitrate, manganese (IV), iron (III), and sulfate). Thermodynamic calculations of anaerobic methanotrophic acetogenesis reactions in aqueous hydrothermal conditions that require oxidized compounds such as sulfur, nitrogen, and iron are considered in Table 1. For example, the free energy of the reaction $\text{CH}_4 + 6\text{Fe}_2\text{O}_3 = 0.5\text{CH}_3\text{COOH} + \text{H}_2\text{O} + 4\text{Fe}_3\text{O}_4$ at 473 K is equal to the sum of the free energy of products formation minus the sum of free energy of the reactants formation at the same temperature ($\Delta G_{473}^0 = (0.5\Delta G_{\text{CH}_3\text{COOH}}^0 + \Delta G_{\text{H}_2\text{O}}^0 + 4\Delta G_{\text{Fe}_3\text{O}_4}^0) - (\Delta G_{\text{CH}_4}^0 + 6\Delta G_{\text{Fe}_2\text{O}_3}^0) = -6.49 \text{ kJ/mol}$).

It is obvious that methane oxidation with nitrogen oxide compounds is thermodynamically very favorable, compared to oxidants such as sulfate, magnetite and hematite. The acetogenesis reactions are energetically more preferable under acidic hydrothermal conditions (the protonated compounds). The change in the free energy with temperature change indicates whether the reaction displays a thermodynamic preference for low-temperature (L) or high-temperature (H) conditions. The reactions of methane with sulfate and iron-oxides is the most thermodynamically favorable with increasing temperature (decreasing ΔG_r^0), whereas the reactions with nitrogen-oxides have different directions. The methane fixation is an energetically more favorable process than CO₂ fixation. For example, in aerobic acetogenesis ($\text{CH}_4 + \text{O}_2 = 0.5\text{CH}_3\text{COOH} + \text{H}_2\text{O}$), more free energy is released in the methane fixation reaction ($\Delta G_{298}^0 = -417.35 \text{ kJ/mol}$ under standard conditions; aqueous constants from [57]) than in the process of CO₂ fixation ($\text{CO}_2 + 2\text{H}_2 = 0.5\text{CH}_3\text{COOH} + \text{H}_2\text{O}$; $\Delta G_{298}^0 = -84.75 \text{ kJ}$).

Table 1. Free Gibbs energy of aqueous reactions of anaerobic methanotrophic acetogenesis at 298 and 473 K at the saturated vapor pressure (P_{SAT}). Redox pairs are the oxidized and reduced states of the oxidant in the reactions. The oxidation of methane to fully ionized and non-ionized forms of acetate is presented. Value of ΔG⁰_T at 298 and 473 K indicates the advantage of the reactions at low (L) or high (H) temperatures. Free energies of aqueous species formation at P_{SAT} (57) were used in calculations

Redox pairs of nitrogen	ΔG⁰₂₉₈ kJ/mol CH₄	ΔG⁰₄₇₃ kJ/mol CH₄	
CH ₄ + 2NO = 0.5CH ₃ COOH + H ₂ O + N ₂	-586.78	-563.18	L
CH ₄ + 2NO = 0.5CH ₃ COO ⁻ + 0,5 H ⁺ + H ₂ O + N ₂	-573.39	-538.33	
CH ₄ + 4NO = 0.5CH ₃ COOH + H ₂ O + 2N ₂ O	-582.32	-535.87	L
CH ₄ + 4NO = 0.5CH ₃ COO ⁻ + 0,5 H ⁺ + H ₂ O + 2N ₂ O	-568.93	-511.02	
CH ₄ + 4HNO ₂ = 0.5CH ₃ COOH + 3H ₂ O + 4NO	-264.46	-320.79	H
CH ₄ + 4NO ₂ ⁻ + 3.5H ⁺ = 0.5CH ₃ COO ⁻ + 4NO + 3H ₂ O	-324.71	-398.7	
CH ₄ + 2HNO ₃ = 0.5CH ₃ COOH + H ₂ O + 2HNO ₂	-295.16	-286.35	L
CH ₄ + 2NO ₃ ⁻ = 0.5CH ₃ COO ⁻ + 2NO ₂ ⁻ + H ₂ O + 0.5H ⁺	-230.07	-217.58	
CH ₄ + 1.33HNO ₃ = 0.5CH ₃ COOH + 1.67H ₂ O + 1.33NO	-286.41	-299.38	H
CH ₄ + 1.33NO ₃ ⁻ + 0.83H ⁺ = 0.5CH ₃ COO ⁻ + 1.33NO + 1.67H ₂ O	-263.12	-304.34	
CH ₄ + 0.8HNO ₃ = 0.5CH ₃ COOH + 1.4H ₂ O + 0.4N ₂	-405.67	-403.98	L
CH ₄ + 0.8NO ₃ ⁻ + 0.3H ⁺ = 0.5CH ₃ COO ⁻ + 0.4N ₂ + 1.4H ₂ O	-386.33	-382.11	
Redox pairs of iron (mineral buffers)			
CH ₄ + 6Fe ₂ O ₃ = 0.5CH ₃ COOH + H ₂ O + 4Fe ₃ O ₄	11.84	-6.49	HH
CH ₄ + 6Fe ₂ O ₃ = 0.5CH ₃ COO ⁻ + 0,5 H ⁺ + H ₂ O + 4Fe ₃ O ₄	25.23	18.36	
CH ₄ + 1.5FeS ₂ + 0.5Fe ₃ O ₄ = 0.5CH ₃ COOH + H ₂ O + 3FeS	44.65	28.85	HH
CH ₄ + 1.5FeS ₂ + 0.5Fe ₃ O ₄ = 0.5CH ₃ COO ⁻ + 0,5 H ⁺ + H ₂ O + 3FeS	58.04	53.7	
CH ₄ + 2Fe ₃ O ₄ + 3SiO ₂ = 0.5CH ₃ COOH + H ₂ O + 3Fe ₂ SiO ₄	57.23	16.19	HH
CH ₄ + 2Fe ₃ O ₄ + 3SiO ₂ = 0.5CH ₃ COO ⁻ + 0,5 H ⁺ + H ₂ O + 3Fe ₂ SiO ₄	70.62	41.04	
Redox pair of sulphur			
CH ₄ + 0.5H ₂ SO ₄ = 0.5CH ₃ COOH + H ₂ O + 0.5H ₂ S	-42.57	-69.93	H
CH ₄ + 0.5SO ₄ ⁻² + 0,5 H ⁺ = 0.5CH ₃ COO ⁻ + H ₂ O + 0.5H ₂ S	-29.18	-45.07	
Carboxy-methano acetogenesis			
CH ₄ + CO ₂ + 2NO + 2H ₂ = CH ₃ COOH + N ₂ +	-671,53	-620,83	L

Redox pairs of nitrogen	ΔG^0_{298} kJ/mol CH ₄	ΔG^0_{473} kJ/mol CH ₄	
2H ₂ O			
CH ₄ + HCO ₃ ⁻ + 2NO + 2H ₂ = CH ₃ COO ⁻ + N ₂ + 3H ₂ O	-680.97	-636.35	
CH ₄ + 0.5CO ₂ + 6Fe ₂ O ₃ + H ₂ = 0.75CH ₃ COOH + 4Fe ₃ O ₄ + 1.5H ₂ O	-30.54	-35.34	H
CH ₄ + 0.5HCO ₃ ⁻ + 6Fe ₂ O ₃ + H ₂ = 0.75CH ₃ COO ⁻ + 4Fe ₃ O ₄ + 2H ₂ O + 0,25H ⁺	-28.56	-30.64	
CH ₄ +CO ₂ = CH ₃ COOH	24.27	39.89	L
CH ₄ + HCO ₃ ⁻ = CH ₃ COO ⁻ + H ₂ O	14.83	24.41	
Carboxy- acetogenesis			
CO ₂ + 2H ₂ = 0,5CH ₃ COOH +H ₂ O	-84,75	-57,65	H
HCO ₃ ⁻ + 2H ₂ + 0,5H ⁺ = 0,5CH ₃ COO ⁻ + 2H ₂ O	-107,58	-98.01	

The most favorable reaction CH₄+2NO = 0,5CH₃COOH+H₂O+N₂ (Table 1) can be represented as a model of methanotrophic acetogenesis, which is part of the reverse acetyl-CoA pathway. The second part of this path is the reaction of CO₂ reduction: CO₂+2H₂ = 0,5CH₃COOH+H₂O. In sum, this is a very thermodynamically favorable pathway of carbon fixation in the form CH₄ and CO₂: CH₄+CO₂+2NO+2H₂ = CH₃COOH+N₂+2H₂O. The different stoichiometry of acetogenesis was observed in the archaean Methanosarcina acetivorans, when methane oxidation was associated with the reduction of iron (III) [58]. A reaction is proposed in which four methane molecules are oxidized and two CO₂ molecules are reduced to form three acetate molecules. Increasing the ratio of CH₄ to CO₂ (4CH₄+2CO₂+24Fe₂O₃+4H₂ = 3CH₃COOH+6H₂O+16Fe₃O₄) makes the process of anaerobic acetogenesis more thermodynamically favorable (Table 1, carboxy-methano acetogenesis).

The LUCA era apparently proceeded in an environment with high CO₂ partial pressure, whereas the pre-LUCA period proceeded in a reducing environment with a significant availability of methane. The question thus arises: was this ancestral reverse acetyl-CoA relic pathway the only metabolic CH₄ fixation system, or were there other proto-biochemical mechanisms for the assimilation of carbon? .

In addition to the acetyl-CoA pathway, autocatalytic CO₂ fixation cycles have been suggested as the first metabolic autocatalytic systems on early Earth [1,3,59-65]. These include an autocatalytic reductive tricarboxylic acids (rTCA) cycle (reverse citrate cycle, Arnon cycle), a 3-hydroxypropionate cycle, a 3-hydroxypropionate/4-hydroxybutyrate cycle, a reductive dicarboxylate/4-hydroxybutyrate cycle, and a reducing pentose phosphate (Calvin–Benson–Bassham) cycle. The defined sequences of intermediates of these cycles are modules such that their combination can create a variety of metabolic systems, including the specific pathways of carbon fixation [1,3,64,66-68]. To be considered a possible metabolic alternative, assimilating methane through

autocatalytic cycle intermediates must satisfy the fundamental requirements of thermodynamics.

4. THE PROPOSED METHANE-FUMARATE CYCLE

Based on the hypothesis of primordial anaerobic methanotrophic metabolism origin, we assume that some components and modules of the metabolic cycles (carboxylic and keto acids, and their associations (parageneses)) may also be relicts of ancient methanotrophic metabolism. One of the few known reactions of CH₄ fixation is the formation of 2-methylsuccinate as a result of the reaction: fumarate+CH₄ → 2-methylsuccinate [69-71], and fumarate addition has been widely proposed as an initial step in the anaerobic oxidation of both aromatic and aliphatic hydrocarbons [72]. The reaction of methane with fumarate satisfies the “minimal energy requirements” for autotrophic growth [73], and we consider the possibility of its participation in nascent autotrophic metabolism. We propose a simplified model of the methane-fumarate (MF) cycle, Fig. 2, which could have originated in the reductive Archean hydrothermal systems, at a high partial pressure of endogenous methane (facies II, Fig. 1). The cycle is initiated by the reaction of fumarate + methane → 2-methylsuccinate. In the hydration and dehydrogenation or anaerobic oxidation reactions, 2-methylsuccinate is converted to citramalate, which is disproportionated to acetate and pyruvate with cleavage of a carbon-carbon bond. Pyruvate is an important “hub” metabolite that is a precursor for amino acids, carbohydrates, cofactors, and lipids in an extant metabolic network. The following carbon assimilation reaction in the form of CO₂ with the formation of oxaloacetate is a biomimetic analogue of the reductive tricarboxylic acid (rTCA) cycle reaction. An α-carboxylation of pyruvate is a critical anabolic pathway in modern biochemistry, which resupplies rTCA cycle intermediates. Oxaloacetate is transformed into fumarate in the reactions of the citrate cycle intermediates. The resulting fumarate assimilates methane and begins a new MF cycle, in one turnover of which an acetate molecule is formed from methane and carbon dioxide molecules: CH₄+CO₂ = CH₃COOH, Table 1. The nonenzymatic flow of some reaction sequences of the rTCA cycle, such as oxaloacetate → malate → fumarate → succinate has been recently experimentally confirmed [74].

Transformation of fumarate into 2-methylsuccinate introduces into the cycle five-carbon intermediates, such as citramalate and mesaconate, functioning, for example, in the reductive 3-hydroxypropionate CO₂ fixation cycle. The autocatalytic nature of the cycle is due to the presence of a branch point associated with the cleavage of citramalate, and can be described by the reaction of doubling its intermediates in one turn of the cycle: C₄H₆O₅ (malate)+1,5CH₄+2,5CO₂ = 2C₄H₆O₅ (two malates). The most important advantage of the reproduction of the cycle is the complete independence of its functioning from the chemical potentials of molecular hydrogen and water. This type of autotrophic metabolism, as in the case of the acetyl-CoA pathway, can be defined as carboxy-methanotrophic acetogenesis. As it happened with the archaean WL pathway (eg, [58]), methanotrophy probably should be combined with the carboxylation process, therefore nature had to look for all possible

sources of carbon dioxide. The problem of the most energetically unfavorable reaction of 2-methylsuccinate transformation into citramalate ($\Delta G^0_{298} = 96.57$ kJ), Table 2, can be solved by using oxidants, such as oxides of nitrogen and iron (Fig. 2, inset). Nitric oxide (NO) is the strongest oxidant, but the reaction with Fe_2O_3 is also favorable at physiological temperatures.

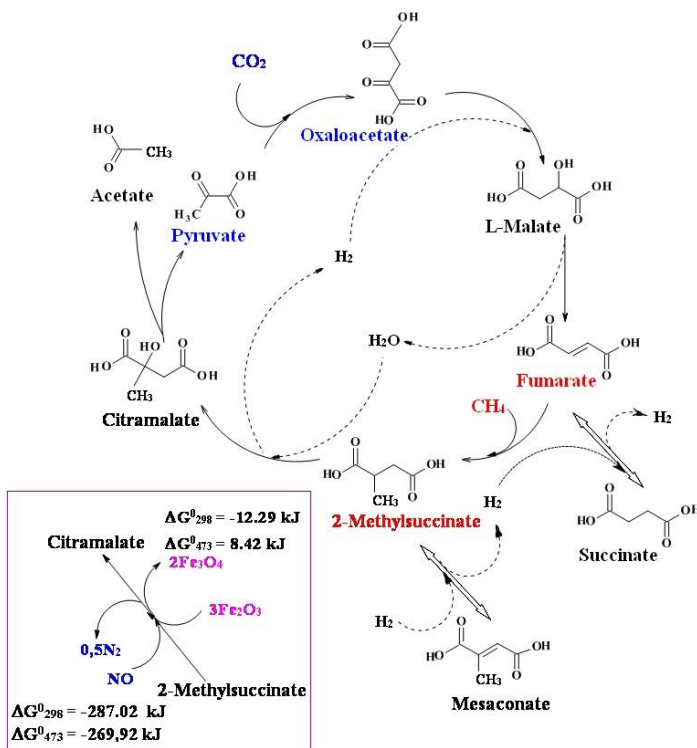


Fig. 2. The scheme of the proposed methane-fumarate (MF) cycle. Carbon from methane is introduced into the fumarate (marked by red), and from CO_2 into the pyruvate (marked by blue) with the formation of a C–C bond. The reaction sequence pyruvate \rightarrow oxaloacetate \rightarrow fumarate \rightarrow succinate is part of the reductive tricarboxylic acid (rTCA) cycle, an enzyme-free archaic version of which is proposed as the basis of ancient autotrophic metabolism (59; 60). The inset shows options for the oxidative transformation of 2-methylsuccinate to citramalate with hematite (Fe_2O_3) and nitric oxide (NO) as oxidants. The chemical potential of hydrogen in the environment determines the equilibrium shift in the reactions succinate \leftrightarrow fumarate and 2-methyl succinate \leftrightarrow mesaconate

The reversibility of the reactions in the citrate cycle is mainly determined by the equilibrium of fumarate+H₂ = succinate ($\Delta G^0_{298} = -102.24$, $\Delta G^0_{473} = -88.88$ kJ), Table 2. The change in the direction of electron flow therein is determined by the chemical potential of hydrogen [61], and therefore, different proto-metabolic cycles could be formed, for example, the oxidative citrate and reductive 3-hydroxypropionate cycles (succinate → fumarate), the rTCA cycle (fumarate → succinate), or the proposed CH₄ fixation cycle (succinate → fumarate → 2-methylsuccinate).

Anaerobic methane-oxidizing branch of cycle represents the transformation of fumarate to pyruvate and acetate. The free energies of these reactions with various inorganic oxidizing agents at 298 and 473 K are given in Table 2. Assimilation of CH₄ in the oxidizing branch of the cycle, Fig. 2, demonstrates highly favorable thermodynamics with all redox pairs of nitrogen. The same reaction with the iron redox pair becomes more favorable at an increasing temperature. Reactions with iron mineral buffers, Table 2, are closer to the equilibrium state, which ultimately determines the possibilities of primordial cycle flow in the forward or reverse directions (development of methanogenesis or methanotrophic acetogenesis). An analysis of the oldest known association of microfossils suggests that methane-cycling methanogen-methanotroph communities were a significant component of the earth's early biosphere [75]. It is possible that a high methane partial pressure which existed in a geodynamic regime of high endogenous methane flow in ancient Earth, promoted the formation of various versions of carbon assimilating systems.

Table 2. The free energy of reactions of MF cycle (a) and reactions of its anaerobic oxidative branch (b) with different oxidants at 298 and 473 K and P_{SAT}. For comparison, the reaction of methane oxidation with molecular oxygen is considered. Free energies of aqueous substances formation at P_{SAT} [57,62] (El. Suppl. Mat.), [76] were used in calculations

a. Reactions of cycle		ΔG^0_{298} kJ/mol	ΔG^0_{473} kJ/mol	
1.	(CH) ₂ (COOH) ₂ (fumarate) + CH ₄ = (CH ₂)(CH ₃ CH)(COOH) ₂ (2-methylsuccinate)	-44.95	-29.97	L
2.	(CH ₂)(CH ₃ CH)(COOH) ₂ + H ₂ O = (CH ₃ CH)CH(OH)(C OOH) ₂ (citramalate) + H ₂	96.57	94.14	H
3.	(CH ₃ CH)CH(OH)(COOH) ₂ = CH ₃ COOH (acetate) + CH ₃ (CO)COOH (pyruvate)	19.35	1.73	H
4.	CH ₃ (CO)COOH + CO ₂ = CH ₂ CO(COOH) ₂ (oxaloacetate)	13.11	35.03	L
5.	CH ₂ CO(COOH) ₂ + H ₂ = CH ₂ CH(OH)(COOH) ₂ (malate)	-65.49	-55.78	L
6.	CH ₂ CH(OH)(COOH) ₂ = (CH) ₂ (COOH) ₂ + H ₂ O	5.68	-5.26	H
7.	(CH) ₂ (COOH) ₂ (fumarate) + H ₂ = (CH ₂) ₂ (COOH) ₂ (succinate)	-102.24	-88.88	L
8.	(CH ₃ C=CH)(COOH) ₂ (mesaconate) + H ₂ = (CH ₂)(CH ₃ CH)(COOH) ₂	-66.53	-54.85	L

a. Reactions of cycle	ΔG^0_{298} kJ/mol	ΔG^0_{473} kJ/mol	
b. Oxidative reactions of cycle methane branch	ΔG^0_{298} kJ/mol	ΔG^0_{473} kJ/mol	
(CH) ₂ (COOH) ₂ (fumarate) + CH ₄ + H ₂ O = CH ₃ COOH (acetate) + CH ₃ (CO)COOH (pyruvate) + H ₂	70.97	65.9	H
(CH) ₂ (COOH) ₂ + CH ₄ + 0.5O ₂ = CH ₃ COOH + CH ₃ (CO)COOH	-192.22	-182.53	L
(CH) ₂ (COOH) ₂ + CH ₄ + Fe ₃ O ₄ + 1.5SiO ₂ = CH ₃ COOH + CH ₃ (CO)COOH + 1.5Fe ₂ SiO ₄	45.08	25.21	H
(CH) ₂ (COOH) ₂ + CH ₄ + 3Fe ₂ O ₃ = CH ₃ COOH + CH ₃ (CO)COOH + 2Fe ₃ O ₄	22.38	13.87	H
(CH) ₂ (COOH) ₂ + CH ₄ + 0.75FeS ₂ + 0.25Fe ₃ O ₄ = CH ₃ COOH + CH ₃ (CO)COOH + 1.5FeS	38.78	31.54	H
(CH) ₂ (COOH) ₂ + CH ₄ + 2HNO ₂ = CH ₃ COOH + CH ₃ (CO)COOH + H ₂ O + 2NO	-115.77	-143.28	H
(CH) ₂ (COOH) ₂ + CH ₄ + 2NO = CH ₃ COOH + CH ₃ (CO)COOH + N ₂ O	-274.7	-250.83	L
(CH) ₂ (COOH) ₂ + CH ₄ + NO = CH ₃ COOH + CH ₃ (CO)COOH + 0.5N ₂	-276.93	-264.48	L

Methyl group formation by the oxidation of methane is limited by kinetics, because the dissociation energy of the C–H bond in methane (439 kJ) exceeds that of the X–H bond in other organic molecules, with the exception of the O–H bond in H₂O (497 kJ) and other oxygen-derived molecular species. In the field of alkane oxidation, enzymatic metal-oxo species, promote C–H activation through a metallo-radical pathway. This involves hydrogen radical abstraction from the alkane by the oxo species, followed by a rapid rebound of the radical species onto the metal hydroxo intermediate [77,78]. The calculation of the potential energy surface showed the thermodynamic possibility of anaerobic oxidation of methane via fumarate addition, in a reaction catalyzed by the glycol radical [73]. The reaction mechanism fumarate+CH₄ → 2-methylsuccinate, Fig. 2, seems to be similar to the radical mechanism of breaking the C–H bond with the formation of the C–C bond, catalyzed by benzylsuccinate synthase [79,80] during microbiological fixation of toluene by fumarate. Radicals of amino acids and dipeptides may be the possible catalysts of methane activation with the formation of methyl radical as an attacking agent. The formation of pyruvate and oxaloacetate in MF cycle, Fig. 2, indicates a very likely formation of amino acids in simple aqueous synthesis, for example: C₃H₄O₃ (pyruvate)+NH₃ = C₃H₇O₃N (serine), $\Delta G^0_{298} = -10,10$ kJ or pyruvate+NH₃+H₂ = C₃H₇NO₂(alanine)+H₂O, $\Delta G^0_{298} = -124,8$ kJ. Barge et al. [81] show that pyruvate can form the alanine in hydrothermal systems in the presence of mixed-valence iron oxyhydroxides. Moreover, the generation of reactive oxygen species H₂O₂ and OH[•] from minerals and H₂O in anaerobic environments (eg. [82]) creates the possibility of various radical mechanisms for the oxidation of substrates in a hydrothermal environment. According to [83], LUCA metabolism had an excess of radical reaction mechanisms, which, in our opinion, could also participate in the reaction

of CH₄ fixation in the cycle, overcoming the activation barriers of kinetically unfavorable reaction steps.

Our understanding of the emergence of methanotrophic metabolism is within the framework of the hydrothermal theory for the origin of life (eg, [84]) with all its advantages (continuous flow of energy and matter, the temperature gradient, great possibilities of homogeneous and heterogeneous metal catalysis). Before the occurrence of cellular structures, the primary autotrophic metabolism on the surface of minerals created the chemical space of competing autocatalytic carbon fixation cycles. Regardless of the specific mechanism of the functioning of the precellular autotrophic metabolism ("reductive surface pyrite world" [85], "hydrothermal reactor" [86], and others) its origin and development was subject to the laws of aqueous thermodynamics.

5. ANAEROBIC METHANE OXIDATION IN THE HYDROTHERMAL SYSTEMS

We represent the hydrothermal system in the form of a phase diagram which displays the chemical potential of oxygen vs. temperature at saturated vapor pressure (P_{SAT}), where temperatures and pressures are below critical thresholds (647,3 K and 22,1 MPa) (Fig. 3). The chemical potentials (μ_i) of components representing its partial energy, the value μ_i is expressed through activity α_i or fugacity f_i as follows: $\mu_i = (\mu_i^0)_{T,p} + RT \ln \alpha_i = (\mu_i^0)_{T,p} + RT \ln f_i$. Here numerical values depend on conventional standard states. For activity, the state of pure crystalline substance or unit molal concentration is usually considered as a standard state at a given temperature and pressure. In this state $\alpha_i = 1$ and, hence, $\mu_i = (\mu_i^0)_{T,p}$. The diagram is a two-component system (extensive parameters: C and H), since oxygen become intensive parameters, like the temperature, and pressure. Oxygen is represented by the chemical potential of O₂ in hydrothermal solution ($\mu_{O_2}^P = RT \ln a_{O_2}$, where a_{O_2} denotes the chemical activity of oxygen). According to the Gibbs' phase rule, at arbitrary pressure, the nonvariant equilibria in the diagram (points) consist of four phases, and the three-phase equilibria (lines) divide the divariant stability fields (facies) of the two-phase equilibria.

The equilibrium CH₄+2O₂ = CO₂+2H₂O (bold black line) divides the diagram into the facies of CO₂ (I) and CH₄ (II) (oxic and anoxic areas of the hydrothermal system) and illustrates the two main possibilities for the development of the C–H–O system in the facies carbon dioxide or methane. Intermediates of the MF cycle are acetate, succinate, and fumarate, and we considered their metastable equilibria and parageneses. In all phase space under consideration, there are fumarate facies. The equilibrium of 5Fum+4CH₄+2O₂ = 6Suc at low-temperature (Fig. 3), is located in the region of very low partial pressures of oxygen, whereas the equilibrium of Fum+2CH₄+O₂ = 3Acet at high-temperature occurs in facies of high pressures. Acetate and succinate facies (contoured with red and blue equilibria, respectively) completely encompass the equilibrium of CH₄+O₂ = CO₂+H₂O. That is, in hydrothermal solution, the parageneses of some components within the MF cycle are stable in both the CO₂ and the CH₄ facies. The whole system can develop in either of two directions as the chemical

potential of oxygen changes: formation of low-temperature (Suc-H₂O) and high-temperature (Fum-H₂O) paragenesis in CO₂ facies (I) and formation of low-temperature (Suc-CH₄) and high-temperature (Fum-CH₄) paragenesis in CH₄ facies (II). Thus, within these facies, protobiochemical systems supporting carbon fixation in the form of CO₂ or CH₄ can develop, and methane facies (II) represent a broad area of CH₄ assimilation by carboxylic acids in an aqueous environment. The high stability of the succinate-fumarate-acetate paragenesis in hydrothermal systems at 200° C (473 K) was experimentally shown [88].

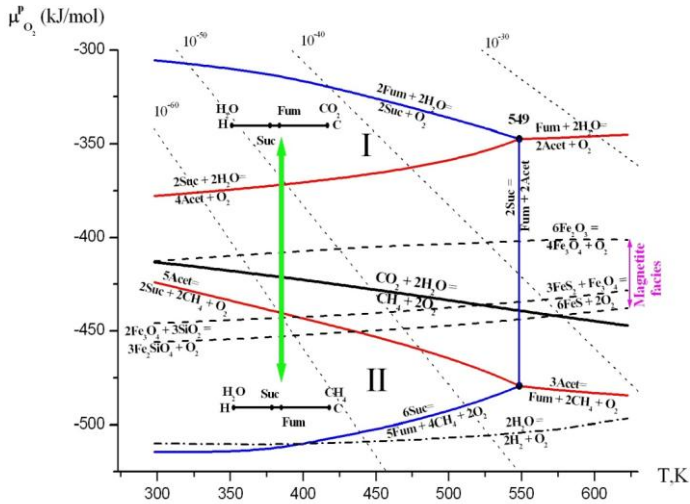


Fig. 3. Diagram of the chemical potential of oxygen ($\mu^P_{O_2}$) - temperature (T, K) at saturated vapor pressure (P_{SAT}). The areas of thermodynamic stability of substances and their parageneses were calculated according to the method described in [61,87]. Points (indicated by temperature values) and lines represent four-phase and three-phase equilibria, separating the two-phase divariant fields of substance stabilities. The bold black line represents the equilibrium of $CO_2 \leftrightarrow CH_4$ and separates their areas of thermodynamic stability (I and II). The dashed lines are equilibria of mineral buffers: hematite-magnetite, Fe_2O_3/Fe_3O_4 (HM), pyrite-pyrrhotite-magnetite, $FeS_2+Fe_3O_4/FeS$ (PPM), and quartz-magnetite-fayalite, $SiO_2+Fe_3O_4/Fe_2SiO_4$ (QMF). The isolines of the activity of O_2 (10^{-n} M, dot lines) are drawn. The acetate and succinate facies are outlined in red and blue equilibria, respectively. We provide only two linear diagrams of the two-component C-H system, denoting the CO_2 and CH_4 facies. The transition between this facies with the change of chemical potential of oxygen is indicated by a green arrow. Abbreviation: Succinate – Suc, Fumarate – Fum, Acetate –Acet

Mineral buffers up to 549 K are located in the facies of succinate, but the equilibrium of HM remains in the area of thermodynamic CO₂ stability (facies I), and PPM and QMF equilibria occur in methane facies II and intersect the fundamental equilibrium of $2\text{Suc} + 2\text{CH}_4 + \text{O}_2 = 5\text{Acet}$. Magnetite (Fe₃O₄) facies (between HM and QMF equilibria) encompass CH₄/CO₂ equilibrium in nearly the entire temperature range of the hydrothermal system under consideration. Thus, the redox areas of magnetite stability correspond to the formation conditions both CO₂ and CH₄ assimilating systems. The presence of magnetite in the early Archean ocean was shown by [89]. Shibuya et al. [90] also conclude that iron redox reactions probably played an important role in the early evolution of methanotrophic metabolisms in the Hadean alkaline hydrothermal system. The QMF buffer equilibrium is completely located in the methane facies (I), which, according to data [18], corresponds on average to the redox conditions of Hadean mantle and crust. Up to the 3.6 billion years ago and maybe even to the great oxidative event of 2.2-2.4 billion years ago on, the earth's surface the oxidation potential of the magnetite redox pairs, apparently, determined the chemical potential of environmental oxygen.

6. CONCLUSION

The cyclic planetary fluid flows (outgassing of volatiles from mantle) drive earth's chemical evolution, leading to the formation of different geobiochemical systems of carbon fixation. Impulses of CO₂ and CH₄ degassing on our planet must have determined the preference of specific autotrophic carbon fixation metabolism development. It is widely accepted that autotrophic metabolism is the fixation of inorganic carbon solely in the form of CO₂, but the origin of methane, both on the ancient Earth, and on the planets and satellites (for example, on Titan) is clearly inorganic; therefore, carbon fixation from methane is also a manifestation of autotrophic metabolism (formation of organic compounds from inorganic precursors).

The variety of modern autotrophic carbon fixation seems to be created by the association of the different metabolic associations and modules that, apparently, could function in the ancestral systems of the anaerobic fixation of CH₄. When approximately ~ 3.6 billion years [18], a CO₂ degassing regime became dominant on our planet, the relic methanotrophy systems were forced to die out or be thrown into unusual and extreme ecological niches. If we consider LUCA as a relatively recent player in the evolution of life [91], the ancestral metabolic systems of carbon fixation in putative pre-LUCA could differ appreciably from modern ones.

In the process of development of CO₂ fixation systems on the Earth, the main problem was the presence of electron donors (therefore, evolution created selective reducing agents: NADH, NADPH, FADH), whereas the fixation of CH₄ essentially depended on the presence of electron acceptors. The oxygen-containing nitrogen compounds are the best oxidants in the hydrothermal systems, but their presence there is problematic [92]. Nevertheless, the redox pairs of hematite-magnetite and quartz-magnetite-fayalite create a specific area

of chemical potential of oxygen that satisfies the thermodynamic requirements of oxidation and assimilation of methane by protometabolic pathways. Hydrothermal systems of ancient Earth may have been very similar to those that currently exist on some extraterrestrial cosmic bodies, such as Europa or Enceladus. The degassing of these cosmic bodies can currently support methane metabolism, but the problem is to know if there are electron acceptors there [93].

ACKNOWLEDGEMENTS

The work was carried out within the framework of the state task of the Federal Research Center for Problems of Chemical Physics and Medical Chemistry, RAS, state registration number AAAA-A19-119071190045-0.

COMPETING INTERESTS

Authors have declared that no competing interests exist.

REFERENCES

1. Braakman R, Smith E. The emergence and early evolution of biological carbon-fixation. *PLOS Comput Biol.* 2012;8(4):e1002455.
2. Goldford JE, Hartman H, Smith TF, Segrè D. Remnants of an ancient metabolism without phosphate. *Cell.* 2017;168(6):1126-1134.e9.
3. Marakushev SA, Belonogova OV. Chemical basis of carbon fixation autotrophic paleometabolism. *Biol Boll Russ Acad Sci.* 2021b;48(5):519-29.
4. Marakushev SA. Transformation of hydrocarbons into components of archaic chemoautotrophic CO₂ fixation cycle. *Dokl Biochem Biophys.* 2008;418:18-23.
5. Marakushev AA, Marakushev SA. Formation of oil and gas fields. *Lithol Miner Resour.* 2008;43(5):454-69.
6. Marakushev AA, Marakushev SA. Fluid evolution of the Earth and origin of the biosphere. In: Florinsky IV, editor. *Man and the geosphere.* New York: Nova Science Publishers, Inc. 2010;3-31.
7. Marakushev SA, Belonogova OV. Ideas and perspectives: development of nascent autotrophic carbon fixation systems in various redox conditions of the fluid degassing on early Earth. *Biogeosciences.* 2019;16(8):1817-28.
8. Marakushev SA, Belonogova OV. An inorganic origin of the "oil-source" rocks carbon substance. *Georesources.* 2021a;23(3):164-76.
9. Tobie G, Lunine JI, Sotin C. Episodic outgassing as the origin of atmospheric methane on Titan. *Nature.* 2006;440(7080):61-4.
10. Bouquet A, Mousis O, Waite JH, Picaud S. Possible evidence for a methane source in Enceladus' ocean. *Geophys Res Lett.* 2015;42(5):1334-9.
11. Engle AE, Hanley J, Dustrud S, Thompson G, Lindberg GE, Grundy WM et al. Phase diagram for the methane–ethane system and its implications for Titan's lakes. *Planet. Sci J.* 2021;2:118-27.

12. Russell MJ, Nitschke W. Methane: fuel or exhaust at the emergence of life? *Astrobiology*. 2017;17(10):1053-66.
13. Oehler DZ, Etiope G. Methane seepage on Mars: Where to look and why. *Astrobiology*. 2017;17(12):1233-64.
14. Touret JLR. Remnants of early Archaean hydrothermal methane and brines in pillow-breccia from the Isua-Greenstone Belt, West Greenland. *Precambrian Res*. 2003;126(3-4):219-33.
15. Schreiber U, Mayer C, Schmitz OJ, Rosendahl P, Bronja A, Greule M et al. Organic compounds in fluid inclusions of Archean quartz—analogue of prebiotic chemistry on early Earth. *Plos One*. 2017;12(6):e0177570.
16. Tian F, Toon OB, Pavlov AA, De Sterck H. A hydrogen-rich early Earth atmosphere. *Science*. 2005;308(5724):1014-7.
17. Zahnle KJ, Gacesa M, Catling DC. Strange messenger: A new history of hydrogen on Earth, as told by xenon. *Geochim Cosmochim Acta*. 2019;244:56-85.
18. Aulbach S, Woodland AB, Vasilyev P, Galvez ME, Viljoen KS. Effects of low-pressure igneous processes and subduction on Fe³⁺/ZFe and redox state of mantle eclogites from Lacey (*Kaapvaal craton*). *Earth Planet Sci Lett*. 2017;474:283-95.
19. Yang X, Gaillard F, Scaillot B. A relatively reduced Hadean continental crust and implications for the early atmosphere and crustal rheology. *Earth Planet Sci Lett*. 2014;393:210-9.
20. Kuwahara H, Nakada R, Kadoya S, Yoshino T, Irifune T. Hadean mantle oxidation inferred from melting of peridotite under lower-mantle conditions. *Nat Geosci*. 2023;16(5):461-5.
21. Allredge LR. A discussion of impulses and jerks in the geomagnetic field. *J Geophys Res*. 1984;89(B6):4403-12.
22. Larson RL, Olson P. Mantle plumes control magnetic reversal frequency. *Earth Planet Sci Lett*. 1991;107(3-4):437-47.
23. Aubert J, Tarduno JA, Johnson CL. Observations and models of the long-term evolution of earth's magnetic field. *Space Sci Rev*. 2010;155(1-4):337-70.
24. Balashov YA, Glaznev VN. Cycles of alkaline magmatism. *Geochem Int*. 2006;44(3):274-85.
25. Marakushev AA, Marakushev SA. Marakushev, A.A., and Marakushev, S.A. PT facies of elementary, hydrocarbon, and organic substances. *Dokl Earth Sci*. 2006;406(1):141-7.
26. Vitale Brovarone AV, Martinez I, Elmaleh A, Compagnoni R, Chaduteau C, Ferraris C et al. Massive production of abiotic methane during subduction evidenced in metamorphosed ophiocarbonates from the Italian Alps. *Nat Commun*. 2017;8:14134.
27. Tao R, Zhang L, Tian M, Zhu J, Liu X, Liu J et al. Formation of abiotic hydrocarbon from reduction of carbonate in subduction zones: Constraints from petrological observation and experimental simulation. *Geochim Cosmochim Acta*. 2018;239:390-408.
28. Scott HP, Hemley RJ, Mao HK, Herschbach DR, Fried LE, Howard WM et al. Generation of methane in the Earth's mantle: in situ high pressure–

- temperature measurements of carbonate reduction. *Proc Natl Acad Sci U S A*. 2004;101(39):14023-6.
29. Schulte M, Blake D, Hoehler T, McCollom T. Serpentinization and its implications for life on the early Earth and Mars. *Astrobiology*. 2006;6(2):364-76.
 30. Kolesnikov A, Kutcherov VG, Goncharov AF. Methane-derived hydrocarbons produced under upper-mantle conditions. *Nat Geosci*. 2009;2(8):566-70.
 31. Etiope G, Sherwood Lollar B. Abiotic methane on Earth. *Rev Geophys*. 2013;51(2):276-99.
 32. McCollom TM. Laboratory simulations of abiotic hydrocarbon formation in Earth's deep subsurface. *Rev Mineral Geochem*. 2013;75(1):467-94.
 33. Smit KV, Shirey SB, Stern RA, Steele A, Wang W. Diamond growth from C-H-N-O recycled fluids in the lithosphere: Evidence from CH₄ micro-inclusions and $\delta^{13}\text{C}$ - $\delta^{15}\text{N}$ -N content in Marange mixed-habit diamonds. *Lithos*. 2016;265:68-81.
 34. Wang DT, Reeves EP, McDermott JM, Seewald JS, Ono S. Clumped isotopologue constraints on the origin of methane at seafloor hot springs. *Geochim Cosmochim Acta*. 2018;223:141-58.
 35. Potter J, Konnerup-Madsen J. A review of the occurrence and origin of abiogenic hydrocarbons in igneous rocks. In: Petford N, McCaffrey KJW, editors. *Hydrocarbons in crystalline rocks*. Special Publications. London: Geological Society. 2003;214:151-73.
 36. Nivin VA, Treloar PJ, Konopleva NG, Ikorsky SV. A review of the occurrence, form and origin of C-bearing species in the Khibiny alkaline igneous complex, kola Peninsula, NW Russia. *Lithos*. 2005;85(1-4):93-112.
 37. Boehnke P, Bell EA, Stephan T, Trappitsch R, Keller CB, Pardo OS et al. Potassic, high-silica Hadean crust. *Proc Natl Acad Sci U S A*. 2018;115(25):6353-6.
 38. Tarduno JA, Cottrell RD, Davis WJ, Nimmo F, Bono RK. PALEOMAGNETISM. A Hadean to Paleoproterozoic geodynamo recorded by single zircon crystals. *Science*. 2015;349(6247):521-4.
 39. Martin WF, Weiss MC, Neukirchen S, Nelson-Sathi S, Sousa FL. Physiology, phylogeny, and LUCA. *Microb Cell*. 2016;3(12):582-7.
 40. Garcia PS, Gribaldo S, Borrel G. Diversity and evolution of methane-related pathways in archaea. *Annu Rev Microbiol*. 2022;76:727-55.
 41. Liu J, Harris RL, Ash JL, Ferry JG, Krause SJE, Labidi J et al. Reversibility controls on extreme methane clumped isotope signatures from anaerobic oxidation of methane. *Geochim Cosmochim Acta*. 2023;348:165-86
 42. Hinrichs KU, Hayes JM, Sylva SP, Brewer PG, DeLong EF. Methane-consuming archaeobacteria in marine sediments. *Nature*. 1999;398(6730):802-5.
 43. Knittel K, Boetius A. Anaerobic oxidation of methane: Progress with an unknown process. *Annu Rev Microbiol*. 2009;63:311-34.
 44. Ettwig KF, Butler MK, Le Paslier D, Pelletier E, Mangenot S, Kuypers MM et al. Nitrite-driven anaerobic methane oxidation by oxygenic bacteria. *Nature*. 2010;464(7288):543-8.

45. Haroon MF, Hu S, Shi Y, Imelfort M, Keller J, Hugenholtz P et al. Anaerobic oxidation of methane coupled to nitrate reduction in a novel archaeal lineage. *Nature*. 2013;500(7464):567-70.
46. Beal EJ, House CH, Orphan VJ. Manganese- and iron-dependent marine methane oxidation. *Science*. 2009;325(5937):184-7.
47. Ettwig KF, Zhu B, Speth D, Keltjens JT, Jetten MSM, Kartal B. Archaea catalyze iron-dependent anaerobic oxidation of methane. *Proc Natl Acad Sci U S A*. 2016;113(45):12792-6.
48. Oni OE, Friedrich MW. Metal oxide reduction linked to anaerobic methane oxidation. *Trends Microbiol*. 2017;25(2):88-90.
49. He Z, Zhang Q, Feng Y, Luo H, Pan X, Gadd GM. Microbiological and environmental significance of metal-dependent anaerobic oxidation of methane. *Sci Total Environ*. 2018;610-611:759-68.
50. Martinez-Cruz K, Leewis MC, Herriott IC, Sepulveda-Jauregui A, Anthony KW, Thalasso F et al. Anaerobic oxidation of methane by aerobic methanotrophs in sub-Arctic lake sediments. *Sci Total Environ*. 2017;607-608:23-31.
51. Timmers PHA, Welte CU, Koehorst JJ, Plugge CM, Jetten MSM, Stams AJM. Reverse methanogenesis and respiration in methanotrophic archaea. *Archaea*. 2017;17:1-22.
52. McGlynn SE. Energy metabolism during anaerobic methane oxidation in ANME Archaea. *Microbes Environ*. 2017;32(1):5-13.
53. Scheller S, Goenrich M, Boecher R, Thauer RK, Jaun B. The key nickel enzyme of methanogenesis catalyses the anaerobic oxidation of methane. *Nature*. 2010;465(7298):606-8.
54. Smejkalová H, Erb TJ, Fuchs G. Methanol assimilation in *Methylobacterium extorquens* AM1: demonstration of all enzymes and their regulation. *Plos One*. 2010;5(10):e13001.
55. Semrau JD, DiSpirito AA, Murrell JC. Life in the extreme: thermoacidophilic methanotrophy. *Trends Microbiol*. 2008;16(5):190-3.
56. Nitschke W, Russell MJ. Beating the acetyl-CoA pathway to the origin of life. *Philos Trans R Soc Lond B Biol Sci*. 2013;368(1622):20120258.
57. Amend JP, Shock EL. Energetics of overall metabolic reactions of thermophilic and hyperthermophilic Archaea and Bacteria. *FEMS Microbiol Rev*. 2001;25(2):175-243.
58. Soo VWC, McAnulty MJ, Tripathi A, Zhu F, Zhang L, Smith PB et al. Reversing methanogenesis to capture methane for liquid biofuel precursors. *Microb Cell Factories*. 2016;15:11.
59. Wächtershäuser G. Evolution of the first metabolic cycles. *Proc Natl Acad Sci U S A*. 1990;87(1):200-4.
60. Smith E, Morowitz HJ. Universality in intermediary metabolism. *Proc Natl Acad Sci U S A*. 2004;101(36):13168-73.
61. Marakushev SA, Belonogova OV. The parageneses thermodynamic analysis of chemoautotrophic CO₂ fixation archaic cycle components, their stability and self-organization in hydrothermal systems. *J Theor Biol*. 2009;257(4):588-97.

62. Marakushev SA, Belonogova OV. The divergence and natural selection of autocatalytic primordial metabolic systems. *Orig Life Evol Biosph.* 2013;43(3):263-81.
63. Fuchs G. Alternative pathways of carbon dioxide fixation: Insights into the early evolution of life? *Annu Rev Microbiol.* 2011;65:631-58.
64. Braakman R, Smith E. The compositional and evolutionary logic of metabolism. *Phys Biol.* 2013;10(1):011001.
65. Xiao L, Liu G, Gong F, Zhu H, Zhang Y, Cai Z et al. A minimized synthetic carbon fixation cycle. *ACS Catal.* 2022;12(1):799-808.
66. Lorenz DM, Jeng A, Deem MW. The emergence of modularity in biological systems. *Phys Life Rev.* 2011;8(2):129-60.
67. Marakushev SA, Belonogova OV. Metabolic design and biomimetic catalysis of the archaic chemoautotrophic CO₂ fixation cycle. *Mos. Univer. Chem Bull.* 2010;65:212-8.
68. Marakushev SA, Belonogova OV. The chemical potentials of hydrothermal systems and the formation of coupled modular metabolic pathways. *Biophysics.* 2015;60(4):542-52.
69. Thauer RK, Shima S. Methane as fuel for anaerobic microorganisms. *Ann N Y Acad Sci.* 2008;1125:158-70.
70. Haynes CA, Gonzalez R. Rethinking biological activation of methane and conversion to liquid fuels. *Nat Chem Biol.* 2014;10(5):331-9.
71. Thauer RK. Methyl (alkyl)-coenzyme M reductases: Nickel F-430-containing enzymes involved in anaerobic methane formation and in anaerobic oxidation of methane or of short chain alkanes. *Biochemistry.* 2019;58(52):5198-220.
72. Musat F. The anaerobic degradation of gaseous, nonmethane alkanes - From in situ processes to microorganisms. *Comput Struct Biotechnol J.* 2015;13:222-8.
73. Beasley KK, Nanny MA. Potential energy surface for anaerobic oxidation of methane via fumarate addition. *Environ Sci Technol.* 2012;46(15):8244-52.
74. Muchowska KB, Varma SJ, Chevallot-Beroux E, Lethuillier-Karl L, Li G, Moran J. Metals promote sequences of the reverse Krebs cycle. *Nat Ecol Evol.* 2017;1(11):1716-21.
75. Schopf JW, Kitajima K, Spicuzza MJ, Kudryavtsev AB, Valley JW. SIMS Anal Oldest Known Assemblage Microfossils document their taxon-correlated carbon isotope compositions *Proc. Natl. Acad. Sci. USA.* 2017;115:53-8.
76. Marakushev SA, Belonogova OV. Thermodynamic factors of natural selection in autocatalytic chemical systems. *Dokl Biochem Biophys.* 2012;444:131-6.
77. Roudesly F, Oble J, Poli G. Metal-catalyzed C H activation/functionalization: The fundamentals. *J Mol Cat A Chem.* 2017;426:275-96.
78. Andrade LS, Lima HHLB, Silva CTP, Amorim WLN, Poço JGR, López-Castillo A et al. Metal-organic frameworks as catalysts and biocatalysts for methane oxidation: the current state of the art. *Coord Chem Rev.* 2023;481:215042.

79. Buckel W, Golding BT. Radical enzymes in anaerobes. *Annu Rev Microbiol.* 2006;60:27-49..
80. Austin RN, Groves JT. Alkane-oxidizing metallo enzymes in the carbon cycle. *Metallomics.* 2011;3(8):775-87.
81. Barge LM, Flores E, Baum MM, VanderVelde DG, Russell MJ. Redox and pH gradients drive amino acid synthesis in iron oxyhydroxide mineral systems. *Proc Natl Acad Sci USA.* 2019;116(11):4828-33.
82. Xian H, Zhu J, Tan W, Tang H, Liu P, Zhu R et al. The mechanism of defect induced hydroxylation on pyrite surfaces and implications for hydroxyl radical generation in prebiotic chemistry. *Geochim Cosmochim Acta.* 2019;244:163-72.
83. Weiss MC, Sousa FL, Mrnjavac N, Neukirchen S, Roettger M, Nelson-Sathi S et al. The physiology and habitat of the last universal common ancestor. *Nat Microbiol.* 2016;1(9):16116.
84. Martin W, Baross J, Kelley D, Russell MJ. Hydrothermal vents and the origin of life. *Nat Rev Microbiol.* 2008;6(11):805-14.
85. Wächtershäuser G. Before enzymes and templates: Theory of surface metabolism. *Microbiol Rev.* 1988;52(4):452-84.
86. Russell MJ, Martin W. The rocky roots of the acetyl-CoA pathway. *Trends Biochem Sci.* 2004;29(7):358-63.
87. Korzhinskii DS. *Physicochemical basis of the analysis of the paragenesis of minerals.* New York: Consultants Bureau, Inc, and London: Chapman & Hall; 1959.
88. Estrada CF, Mamajanov I, Hao J, Sverjensky DA, Cody GD, Hazen RM. Aspartate transformation at 200°C with brucite [Mg(OH)₂], NH₃, and H₂: implications for prebiotic molecules in hydrothermal systems. *Chem Geol.* 2017;457:162-72.
89. Li Y, Konhäuser KO, Zhai M. The formation of magnetite in the early Archean oceans. *Earth Planet Sci Lett.* 2017;466:103-14.
90. Shibuya T, Russell MJ, Takai K. Free energy distribution and hydrothermal mineral precipitation in Hadean submarine alkaline vent systems: importance of iron redox reactions under anoxic conditions. *Geochim Cosmochim Acta.* 2016;175:1-19.
91. Cornish-Bowden A, Cárdenas ML. Life before LUCA. *J Theor Biol.* 2017;434:68-74.
92. Ranjan S, Todd ZR, Rimmer PB, Sasselov DD, Babbitt AR. Nitrogen oxide concentrations in natural waters on early Earth. *Geochem Geophys Geosyst.* 2019;20(4):2021-39.
93. Russell MJ, Murray AE, Hand KP. The possible emergence of life and differentiation of a shallow biosphere on irradiated icy worlds: the example of Europa. *Astrobiology.* 2017;17(12):1265-73.

Biography of author(s)



Sergey A. Marakushev

Federal Research Center for Problems of Chemical Physics and Medical Chemistry, Russian Academy of Sciences, Academician Semenov Avenue 1, Chernogolovka, Moscow Region-142432, Russian Federation.

He was born in 1952, graduated in 1975 from the Faculty of Biology of Moscow State University with a degree in biochemistry. Then he worked in a department of the Institute of Chemical Physics of the USSR Academy of Sciences, where in 1982, he defended his Ph.D. in the specialty of biophysics. From 1984 to 1995, he worked as head of the laboratory of geomicrobiology at the Amur Complex Research Institute of the Far Eastern Branch of the Russian Academy of Sciences in Blagoveshchensk, where he created and substantiated a new scientific trend - geological microbiology and biochemistry of gold, and published the results in a monograph and numerous papers. In 1997, he defended his doctoral dissertation in the specialty biogeochemistry. Since 1995, he has been working at the Institute of Problems of Chemical Physics of Russian Academy of Sciences in Chernogolovka (since 2022, the Federal Research Center for Problems of Chemical Physics and Medical Chemistry RAS). He has developed a biomimetic analysis and a thermodynamic method of organic and mineral parageneses in hydrothermal solutions, which are successfully used in studies of the primary metabolic systems emergence in the process of the origin of life on early Earth, as well as in studies of an inorganic genesis of petrogenic carbon reservoirs (oil deposits, natural gas, oil shale, bitumen, etc.) in the earth's crust. His main areas of research at present are the fixation of carbon dioxide (CO₂) and oxidation of hydrocarbons in the physicochemical conditions of biosphere and geospheres. He is the author of more than 300 peer-reviewed articles, conference thesis's, chapters of collective monographs, as well as two monographs.



Ol'ga V. Belonogova

Federal Research Center for Problems of Chemical Physics and Medical Chemistry, Russian Academy of Sciences, Academician Semenov Avenue 1, Chernogolovka, Moscow Region-142432, Russian Federation.

She was born in 1947, graduated in 1970 Moscow State University, in chemistry, has been working at the FRC PCP MC RAS since 1970, researcher, in 1978 defended Ph.D. of chemical sciences on the topic: "Study of the dynamic structure of globular and fibrial proteins using spin and gamma-resonance labels". She is a qualified specialist in the field of application of physico-chemical methods in biophysics and related fields. She developed an actual scientific direction - the study of the relationship between the functions and dynamics of proteins using spin, Mössbauer and luminescent labels. She carried out

research on the synthesis and characterization of protein-based metal-containing clusters, on the study of the molecular dynamic properties of protein and membrane systems and their relationship with functional activity (electron phototransfer), on the use of spin and luminescent labels to study the conformational state of a number of enzymes and immobilized proteins. In recent years, she has been involved in the development of biomimetic approaches to study the catalytic mechanisms and kinetics of reactions of hydrocarbon oxidation and CO₂ fixation by intermediates in autocatalytic networks, as well as the influence of the supramolecular organization of the chemical space on these processes, applying the method of thermodynamic potentials in aqueous solutions to the abiogenic synthesis of organic compounds in hydrothermal systems. She is the author of more than 80 scientific papers published in peer-reviewed domestic and foreign journals WOS.

© Copyright (2023): Author(s). The licensee is the publisher (B P International).

DISCLAIMER

This chapter is an extended version of the article published by the same author(s) in the following journal. Biogeosciences, 16: 1817–1828, 2019. Available: <https://doi.org/10.5194/bg-16-1817-2019>

Peer-Review History: During review of this manuscript, double blind peer-review policy has been followed. All manuscripts are thoroughly checked to prevent plagiarism. Minimum two peer-reviewers reviewed each manuscript. After review and revision of the manuscript, the Book Editor approved only quality manuscripts for final publication.